10-1-2016

Development and Application of a Standstill Parameter Identification Technique for the Synchronous Generator

Ahmed M.A. Oteafy
Alfaisal University

John N. Chiasson
Boise State University

Said Ahmed-Zaid
Boise State University

Publication Information

Oteafy, Ahmed M.A.; Chiasson, John N.; and Ahmed-Zaid, Said. (2016). "Development and Application of a Standstill Parameter Identification Technique for the Synchronous Generator". *International Journal of Electrical Power & Energy Systems, 81*, 222-231. http://dx.doi.org/10.1016/j.ijepes.2016.02.030

Development and Application of a Standstill Parameter Identification Technique for the Synchronous Generator

Ahmed M. A. Oteafy, John N. Chiasson, and Said Ahmed-Zaid

***Abstract*—This work presents the development of an offline standstill estimation technique, where the synchronous machine is locked at an arbitrary (but known) angle and is excited over a short period of time. The proposed time domain method requires few seconds of captured data in contrast to the well-known standard Standstill Frequency Response (SSFR) technique that could take more than 6 hours to conduct. This is based on nonlinear least squares estimation and algebraic elimination theory. The resulting algorithm is non-iterative where the data is used to construct polynomials that are solved for a finite number of roots which determine the electrical parameter values. Experimental results are presented showing the efficacy of the technique in furnishing the parameters of a salient pole synchronous machine.**

***Index Terms*—Algebraic Elimination Theory, Offline Parameter Identification, Standstill tests, Synchronous Generators.**

I. Introduction

THE field of parameter estimation is an important area of research because it is applicable to many practical engineering problems. Here, we specifically look at the problem of identifying the electrical parameters of large synchronous machines (whether operated as generators or motors). This is motivated by the fact that power system stability analyses (voltage stability, large angle stability, small angle stability, etc.) require accurate parameter values as documented in standards IEEE 1110-2002 [1], IEEE 115-1995 [2], and by supervisory committees such as the Western Electricity Coordinating Council (WECC) in the USA [3]. These analyses are important for real-time monitoring software that alerts system operators to imminent power failures. See reference [4] for a major blackout caused in part by failing to respond to these software tools. Also, accurate knowledge of machine parameters improves the operation of large generators. For example, representing the field circuit dynamics significantly influences the effectiveness of excitation systems as they respond to large rotor angle disturbances (see p. 5 of [1]). Moreover, accurate representations of the field and rotor damper circuits are important for the excitation system to stabilize the machine after small rotor angle disturbances [1].

The synchronous machine model used here represents the rotor with a field winding in the d-axis, and a damper winding in each of the d-axis and q-axis. This is equivalent to Model 2.1 in IEEE 1110-2002 [1]. The parameters of the model can be obtained using standstill *offline* tests, i.e., with the generator disconnected from the grid. These tests, like the standstill frequency response (SSFR) [2], typically use low test voltages to obtain the resistances and unsaturated induction parameters. Other techniques are then used to account for variations due to the operating point temperature and magnetic saturation.

The SSFR is a standard test [1], [2] where a low voltage test signal is applied over a range of frequencies to the stator terminals, with the rotor locked at specific angles/alignments. At each frequency, the stator voltages and currents are measured in steady state. These are used to determine a set of transfer functions representing the synchronous machine [5]. The test is carried out in two parts by aligning the rotor's d-axis with the stator's a-axis and then aligning the rotor's q-axis with the stator's a-axis [6]. By considering the breakpoints in the frequency response, the SSFR test has the capability of identifying the model structure of the machine, specifically, the number of damper windings to be modeled in the d and q axes. The breakpoints, which represent time constants and operational impedances, are related back to the resistors and unsaturated inductances of the appropriate model. Instead, the multitime scale approach by Touhami *et al.* [7] can reduce the model to several simpler transfer functions. As such, the slower dynamics are separated from the faster dynamics and the parameters are obtained from separate tests. Aliprantis *et al.* [8] developed a model of the damper windings as a general transfer function matrix using data collected by the SSFR test. Moreover, their work considers magnetic saturation by lumping its effect into the magnetizing branches. On the other hand, the alignment required by the SSFR test for large generators requires gantry cranes for large adjustments and hand cranks to make minor adjustments in the position, see p. 161 [2]. Bortoni and Jardini in [9] have extended the SSFR technique to allow for the test to be conducted at an arbitrary rotor angle. Their approach was an extension to the earlier work by Dalton and Cameron in [10].

In addition, time domain techniques exist including tests with higher voltage and current levels than the SSFR test, such as the standard short circuit and open circuit tests, see [2], [11]. An example, is the rotating time domain response (RTDR) test by de Mello and Hannett in [12]. There, two of the machine terminals are shorted (b and c) and a field-excitation voltage is applied for a short period of time at lower than rated speeds. The RTDR and SSFR tests were compared in [13] on four

A. Oteafy is with the EE Department, Alfaisal University, PO Box 50927 Riyadh 11533 KSA, aoteafy@alfaisal.edu.

J. Chiasson is with the ECE Department, Boise State University, Boise ID 83725-2075, johnchiasson@boisestate.edu.

S. Ahmed-Zaid is with the ECE Department, Boise State University, Boise ID 83725-2075, sahmedzaid@boisestate.edu.

generators, and the SSFR tests were found to be less expensive to implement and easier to schedule than RTDR tests. Kamwa *et al.* [14] use a PWM excitation with a randomly variable duty ratio applied to the field winding in standstill. The approach obtains the parameter estimates over two stages, first an initial set of operational parameters is found and then the direct parameters are found using the damped Gauss-Newton iterative search algorithm. Also, Tumageanian *et al.* [15], [16] use a step input voltage with the machine in standstill. A maximum likelihood estimation iterative algorithm is used that requires good initial parameter values to ensure convergence. An alternative excitation is the chirp signal which is a sinusoid with linearly increasing frequency. This was used by Cisneros-Gonzalez *et al.* [17] with a hybrid optimization identification technique relying on Genetic algorithms and a Quasi-Newton method.

Conversely, there are *online* estimation methods, i.e., with the machine connected to the grid. An early work by Dandeno *et al.* in [18] applies a supplementary sinusoidal signal to the reference of the automatic voltage regulator (AVR) that results in changes in the field voltage and current. This test is performed while the machine is at 80% of its full load. The data is used to tune the parameters that were previously obtained from an offline SSFR test. Another technique by Tsai *et al.* in [19] injects excitation disturbance voltages into the field winding. Also, in [20] a disturbance in the field excitation reference voltage during online operation is used for their parameter estimation technique. The work in [21] employs a gradient based simulation optimization technique that updates the parameter values based on how closely their simulated response matches recorded data. In [22]–[25] the authors formulate their online estimation method as a nonlinear least-squares problem and solve it through iterative methods. The work of [20] and [26] use maximum likelihood methods, which are also iterative, and assume the process and measurement noise are white for which a Kalman filter type formulation can be used. However, iterative methods have concerns whether they converge or not and, if they do, whether it is to a local or a global minimum.

An approach that does not explicitly inject disturbance signals into the system is presented in [27]; the machine parameters are assumed to be known (using nominal values) and a Luenberger observer is used to estimate the rotor damper winding currents. Using these estimates of the currents, a linear least-squares formulation is then employed to estimate the parameters. The system, including the Luenberger observer, is then updated with the estimated parameter values. However, as the parameters are assumed to be known in order to estimate their values, there is no guarantee that the determined parameters will converge (e.g., in the sense of minimizing a least-squares criterion or some other criteria).

This work presents a standstill test where the stator windings are excited by a balanced three-phase chirp waveform, which sufficiently excites the dynamics of the machine and is continuously differentiable. The stator voltages and currents, and field current are collected over a short period. Using the theory of resultants, an identification model is developed that is directly (non-iteratively) solved for the parameter set that globally minimizes a least-squares criterion. Experimental results are compared with simulation. The methodology was previously applied to develop an identification model for the induction machine in [28]–[35]. The paper expounds on an earlier one [36] by presenting the detailed derivation along with the application of the algorithm. The organization is as follows: Section II gives the machine model and the parameters to be estimated. Section III presents the derivation of the nonlinear parameter identification model. Sections IV and V give the experimental results and the conclusions, respectively.

II. DQ Model of the Synchronous Machine

The nonlinear model of the synchronous machine presented here uses the reference frame adopted by Bergen [37] and Anderson and Fouad [38]. Also, following the approach of Krause [5], the rotor quantities of the machine are scaled using equivalent scaling factors (turn-ratios), but without per-unitization. For more on this model see Ch. 2 of [39]. The synchronous machine reference frame is depicted in Fig. 1.

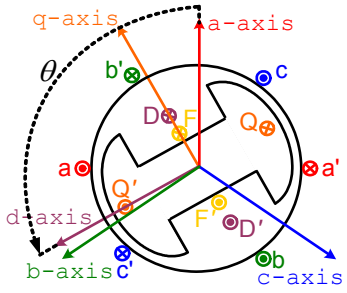

Fig. 1. Schematic representation of a synchronous machine.

The $0dq$ electrical model is given by

$$v_0 = -r_S i_0 - L_{lS}\frac{di_0}{dt} \tag{1}$$

$$v_{Sd} = -r_S i_{Sd} - \omega L_{Sq} i_{Sq} - \omega L_{AQ} i'_{Rq} - L_{Sd}\frac{di_{Sd}}{dt} - L_{AD}\frac{di'_F}{dt} - L_{AD}\frac{di'_{Rd}}{dt} \tag{2}$$

$$v_{Sq} = -r_S i_{Sq} + \omega L_{Sd} i_{Sd} + \omega L_{AD} i'_{Rd} + \omega L_{AD} i'_F - L_{Sq}\frac{di_{Sq}}{dt} - L_{AQ}\frac{di'_{Rq}}{dt} \tag{3}$$

$$-v'_F = -r'_F i'_F - L_{AD}\frac{di_{Sd}}{dt} - L'_F\frac{di'_F}{dt} - L_{AD}\frac{di'_{Rd}}{dt} \tag{4}$$

$$0 = -r'_{Rd} i'_{Rd} - L_{AD}\frac{di_{Sd}}{dt} - L_{AD}\frac{di'_F}{dt} - L'_{Rd}\frac{di'_{Rd}}{dt} \tag{5}$$

$$0 = -r'_{Rq} i'_{Rq} - L_{AQ}\frac{di_{Sq}}{dt} - L'_{Rq}\frac{di'_{Rq}}{dt} \tag{6}$$

The variables of the model are the $0dq$ stator voltages v_0, v_{Sd}, v_{Sq}, the scaled field voltage v'_F, the $0dq$ stator currents i_0, i_{Sd}, i_{Sq}, and the scaled field current i'_F. Other variables include the angle of the rotor θ (in electrical radians) and the angular velocity of the rotor $\omega = d\theta/dt$.

The parameters of the model are the dq stator self inductances L_{Sd}, L_{Sq}, leakage inductance L_{lS} and resistance r_S, the mutual inductances L_{AD}, L_{AQ}, the scaled damper winding

self inductances L'_{Rd}, L'_{Rq} and resistances r'_{Rd}, r'_{Rq}, and the scaled field self inductance L'_F, and resistance r'_F.

The stator variables of the model in the $0dq$ coordinate system are related to their measurable counterparts in the abc coordinate system by a power invariant transformation (In Fig. 1 $v_a = v_{aa'}, v_F = v_{FF'}$) as follows

$$\begin{bmatrix} v_0 \\ v_{Sd} \\ v_{Sq} \end{bmatrix} \triangleq P \begin{bmatrix} v_a \\ v_b \\ v_c \end{bmatrix}, \quad \begin{bmatrix} i_0 \\ i_{Sd} \\ i_{Sq} \end{bmatrix} \triangleq P \begin{bmatrix} i_a \\ i_b \\ i_c \end{bmatrix} \tag{7}$$

with the transformation matrix P defined as

$$P \triangleq \sqrt{\frac{2}{3}} \begin{bmatrix} 1/\sqrt{2} & 1/\sqrt{2} & 1/\sqrt{2} \\ \cos\theta & \cos\left(\theta - \frac{2\pi}{3}\right) & \cos\left(\theta + \frac{2\pi}{3}\right) \\ \sin\theta & \sin\left(\theta - \frac{2\pi}{3}\right) & \sin\left(\theta + \frac{2\pi}{3}\right) \end{bmatrix}.$$

Also, the scaled field rotor variables are related to their measurable counterparts by

$$v'_F \triangleq \frac{1}{N_{afd}} v_F, \; i'_F \triangleq N_{afd} i_F, \tag{8}$$

where N_{afd} is the field winding scaling factor. The damper winding currents are not measurable and therefore it is not necessary (nor possible) to compute their relationship to their scaled counterparts.

The objective of this work is to estimate the resistors and unsaturated inductances of the electrical model, equivalent to IEEE Std. 1110-2002 Model 2.1 [1], namely, r_S, L_{Sd}, L_{Sq}, L_{AD}, L_{AQ}, r'_F, L'_F, r'_{Rd}, L'_{Rd}, r'_{Rq}, and L'_{Rq}. These reduce to nine if L_{lS} is known as $L_{Sd} = L_{lS} + L_{AD}$ and $L_{Sq} = L_{lS} + L_{AQ}$. The standard practice is to rely on the manufacturer supplied value of L_{lS}, see IEEE 1110-2002 [1]. Alternatively, in this work an experiment is conducted to compute its value.

In addition, the field to stator scaling factor N_{afd} is also needed. In practice (see [1]) and in this work, N_{afd} is obtained from the no-load magnetization curve, and relies on an initial estimate of L_{AD} (the manufacturer supplied value). The value of N_{afd} is then used by parameter estimation algorithms to compute L_{AD}, which is typically different from the initial estimate. To resolve this an iterative algorithm was developed in [39] where the value of L_{AD} is used to estimate N_{afd} which in turn is used to re-estimate L_{AD}, etc. until N_{afd} and L_{AD} converge to a consistent pair of values (in the sense that one yields the other). This algorithm is shown to converge from several different initial values of L_{AD}. Another approach is given in [40] for obtaining N_{afd} where its unique characterization is required for modeling magnetic saturation.

III. The Offline Identification Model

At any standstill (fixed) angle θ ($\omega = 0$), with a balanced set of three-phase test voltages, the equations reduce to

$$v_{Sd} = -r_S i_{Sd} - L_{Sd}\frac{di_{Sd}}{dt} - L_{AD}\frac{di'_F}{dt} - L_{AD}\frac{di'_{Rd}}{dt} \tag{9}$$

$$v_{Sq} = -r_S i_{Sq} - L_{Sq}\frac{di_{Sq}}{dt} - L_{AQ}\frac{di'_{Rq}}{dt} \tag{10}$$

$$-v'_F = -r'_F i'_F - L_{AD}\frac{di_{Sd}}{dt} - L'_F\frac{di'_F}{dt} - L_{AD}\frac{di'_{Rd}}{dt} \tag{11}$$

$$0 = -r'_{Rd} i'_{Rd} - L_{AD}\frac{di_{Sd}}{dt} - L_{AD}\frac{di'_F}{dt} - L'_{Rd}\frac{di'_{Rd}}{dt} \tag{12}$$

$$0 = -r'_{Rq} i'_{Rq} - L_{AQ}\frac{di_{Sq}}{dt} - L'_{Rq}\frac{di'_{Rq}}{dt} \tag{13}$$

In DC, the model further reduces to

$$v_{Sd} = -r_S i_{Sd}, \; v_{Sq} = -r_S i_{Sq}, \; v'_F = r'_F i'_F,$$

hence, r_S, and r'_F can be found by simple DC measurements.

We need to obtain a set of independent equations that contain all the parameters and only measurable variables. Towards that end, we solve (12), (13) for di'_{Rd}/dt and di'_{Rq}/dt, substitute them into (9) and (10), and differentiate to obtain two new independent equations

$$\begin{aligned} \frac{dv_{Sd}}{dt} &= -r_S\frac{di_{Sd}}{dt} - L_{Sd}\frac{d^2 i_{Sd}}{dt^2} - L_{AD}\frac{d^2 i'_F}{dt^2} \\ &\quad + L_{AD}^2\frac{1}{L'_{Rd}}\frac{d^2 i_{Sd}}{dt^2} + L_{AD}^2\frac{1}{L'_{Rd}}\frac{d^2 i'_F}{dt^2} + L_{AD}\frac{r'_{Rd}}{L'_{Rd}}\frac{di'_{Rd}}{dt} \end{aligned} \tag{14}$$

$$\begin{aligned} \frac{dv_{Sq}}{dt} &= -r_S\frac{di_{Sq}}{dt} - L_{Sq}\frac{d^2 i_{Sq}}{dt^2} + L_{AQ}^2\frac{1}{L'_{Rq}}\frac{d^2 i_{Sq}}{dt^2} \\ &\quad + L_{AQ}\frac{r'_{Rq}}{L'_{Rq}}\frac{di'_{Rq}}{dt} \end{aligned} \tag{15}$$

Next, we solve (9) and (10) for the unknown variables di'_{Rd}/dt and di'_{Rq}/dt by rearranging them as

$$\frac{di'_{Rd}}{dt} = -\frac{1}{L_{AD}}v_{Sd} - \frac{1}{L_{AD}}r_S i_{Sd} - \frac{1}{L_{AD}}L_{Sd}\frac{di_{Sd}}{dt} - \frac{di'_F}{dt} \tag{16}$$

$$\frac{di'_{Rq}}{dt} = -\frac{1}{L_{AQ}}v_{Sq} - \frac{1}{L_{AQ}}r_S i_{Sq} - \frac{1}{L_{AQ}}L_{Sq}\frac{di_{Sq}}{dt}. \tag{17}$$

Then, we substitute equations (16) and (17) into the two (new) independent equations (14), (15), and into (11) to obtain

$$\begin{aligned} &\frac{dv_{Sd}}{dt} + r_S\frac{di_{Sd}}{dt} + L_{lS}\frac{d^2 i_{Sd}}{dt^2} \\ &= -\left(\frac{d^2 i_{Sd}}{dt^2} + \frac{d^2 i'_F}{dt^2}\right) L_{AD} \\ &\quad - \left(v_{Sd} + r_S i_{Sd} + L_{lS}\frac{di_{Sd}}{dt}\right)\frac{r'_{Rd}}{L'_{Rd}} \\ &\quad + \left(\frac{d^2 i_{Sd}}{dt^2} + \frac{d^2 i'_F}{dt^2}\right) L_{AD}^2\frac{1}{L'_{Rd}} - \left(\frac{di_{Sd}}{dt} + \frac{di'_F}{dt}\right) L_{AD}\frac{r'_{Rd}}{L'_{Rd}} \end{aligned} \tag{18}$$

$$\begin{aligned}&\frac{dv_{Sq}}{dt}+r_S\frac{di_{Sq}}{dt}+L_{lS}\frac{d^2i_{Sq}}{dt^2} \\ &=-\frac{d^2i_{Sq}}{dt^2}L_{AQ}-\left(v_{Sq}+r_Si_{Sq}+L_{lS}\frac{di_{Sq}}{dt}\right)\frac{r'_{Rq}}{L'_{Rq}} \\ &+\frac{d^2i_{Sq}}{dt^2}L_{AQ}^2\frac{1}{L'_{Rq}}-\frac{di_{Sq}}{dt}L_{AQ}\frac{r'_{Rq}}{L'_{Rq}}\end{aligned} \tag{19}$$

$$v'_F-r'_Fi'_F+v_{Sd}+r_Si_{Sd}+L_{lS}\frac{di_{Sd}}{dt}=-\frac{di'_F}{dt}L_{AD}+\frac{di'_F}{dt}L'_F \tag{20}$$

The identification model is based on equations (18), (20) for the d-axis, and (19) for the q-axis. These equations are *nonlinear* in the parameters.

A. Identification of d-axis parameters

Re-writing (18) and (20) in regressor form results in

$$y_d=W_dK_d \tag{21}$$

where

$$y_d\triangleq\begin{bmatrix}\dfrac{dv_{Sd}}{dt}+r_S\dfrac{di_{Sd}}{dt}+L_{lS}\dfrac{d^2i_{Sd}}{dt^2}\\ v'_F-r'_Fi'_F+v_{Sd}+r_Si_{Sd}+L_{lS}\dfrac{di_{Sd}}{dt}\end{bmatrix}$$

$$W_d\triangleq$$

$$\begin{bmatrix}-\dfrac{d^2i_{Sd}}{dt^2}-\dfrac{d^2i'_F}{dt^2} & -v_{Sd}-r_Si_{Sd}-L_{lS}\dfrac{di_{Sd}}{dt} & \dfrac{d^2i_{Sd}}{dt^2}+\dfrac{d^2i'_F}{dt^2} & \dfrac{d^2i_{Sd}}{dt^2}+\dfrac{d^2i'_F}{dt^2} & 0 & -\dfrac{di_{Sd}}{dt}-\dfrac{di'_F}{dt}\\ -\dfrac{di'_F}{dt} & 0 & 0 & 0 & \dfrac{di'_F}{dt} & 0\end{bmatrix},$$

$$K_d=\begin{bmatrix}\kappa_1 & \kappa_2 & \kappa_3 & \kappa_4 & \kappa_5\end{bmatrix}^T \triangleq\begin{bmatrix}L_{AD} & \dfrac{r'_{Rd}}{L'_{Rd}} & L_{AD}^2\dfrac{1}{L'_{Rd}} & L'_F & L_{AD}\dfrac{r'_{Rd}}{L'_{Rd}}\end{bmatrix}^T. \tag{22}$$

where K_d contains the unknown parameters, whereas y_d and W_d are known from the measured variables.

Note that (21) is overparameterized, that is, the parameters making up K_d are not all independent as $\kappa_5=\kappa_1\kappa_2$.

The current and voltage variables are sampled at $t=T$, $2T$, $3T$, ... , NT, where T is the sampling period and N is the total number of samples collected. The derivatives of the variables are computed by numerical differentiation. Then, the elements of vector y_d and the matrix W_d are computed for each data point $n=1$ to N.

One desires to find K_d that minimizes the mean squared error defined by

$$E_d^2(K_d)\triangleq\sum_{n=1}^{N}\left\|y_d(nT)-W_d(nT)K_d\right\|^2. \tag{23}$$

Multiplying out the right-hand side of (23) gives

$$E_d^2(K_d)=R_y-R_{Wy}^TK_d-K_d^TR_{Wy}+K_d^TR_WK_d \tag{24}$$

where

$$R_y\triangleq\sum_{n=1}^{N}y_d^T(nT)y_d(nT),\ R_W\triangleq\sum_{n=1}^{N}W_d^T(nT)W_d(nT),$$

$$R_{Wy}\triangleq\sum_{n=1}^{N}W_d^T(nT)y_d(nT). \tag{25}$$

If R_W were invertible, we would minimize

$$E_d^2(K_d)by\partial E_d^2(K_d)/\partial K_d=-2R_{Wy}+2R_WK_d=0,$$

that is

$$K_d=R_W^{-1}R_{Wy}.$$

However, R_W turns out to be singular regardless of the data collected. Note that

$$W_dM^T=\begin{bmatrix}0 & 0\end{bmatrix}^T,$$

where

$$M\triangleq\begin{bmatrix}1 & 0 & 1 & 1 & 0\end{bmatrix}.$$

Then

$$M\,R_W\,M^T=\sum_{n=1}^{N}M\,W_d^T(nT)W_d(nT)\,M^T=0.$$

Therefore, we *cannot* solve the overparameterized linear regressor for the d-axis parameters.

To address this singularity issue, we reformulate the above overparameterized model as a nonlinear least-squares problem and use algebraic elimination theory to find the solution (see [28]–[35] for other applications of this methodology).

First, we enforce the constraint by substituting $\kappa_5=\kappa_1\kappa_2$ in the error equation,

$$\begin{aligned}&E_p^2(\kappa_1,\kappa_2,\kappa_3,\kappa_4)\\ =\ &R_y-2R_{Wy}^TK_d\big|_{\kappa_5=\kappa_1\kappa_2}+K^TR_WK_d\big|_{\kappa_5=\kappa_1\kappa_2}.\end{aligned} \tag{26}$$

Let R_{Wij} denote the (i,j) element of the matrix R_W, and similarly R_{Wyr} denotes the r^{th} element of the vector R_{Wy} (R_W and R_{Wy} contain the data). The matrix R_W is symmetric so that every $R_{Wij}=R_{Wji}$. Explicitly, we write

$$\begin{aligned}&E_p^2(\kappa_1,\kappa_2,\kappa_3,\kappa_4)\\ &=R_y-2\left(R_{Wy1}\kappa_1+R_{Wy2}\kappa_2+R_{Wy3}\kappa_3\right.\\ &\left.+R_{Wy4}\kappa_4+R_{Wy5}\kappa_1\kappa_2\right)+\kappa_1\left(R_{W11}\kappa_1+R_{W12}\kappa_2\right.\\ &\left.+R_{W13}\kappa_3+R_{W14}\kappa_4+R_{W15}\kappa_1\kappa_2\right)\\ &+\kappa_2\left(R_{W12}\kappa_1+R_{W22}\kappa_2+R_{W23}\kappa_3+R_{W25}\kappa_1\kappa_2\right)\\ &+\kappa_3\left(R_{W13}\kappa_1+R_{W23}\kappa_2+R_{W33}\kappa_3+R_{W35}\kappa_1\kappa_2\right)\\ &+\kappa_4\left(R_{W14}\kappa_1+R_{W44}\kappa_4\right)\\ &+\kappa_1\kappa_2\left(R_{W15}\kappa_1+R_{W25}\kappa_2+R_{W35}\kappa_3+R_{W55}\kappa_1\kappa_2\right)\end{aligned}$$

that only contains the four independent parameters κ_1, κ_2, κ_3, and κ_4.

Note that $E_p^2(\kappa_1,\kappa_2,\kappa_3,\kappa_4)$ is a polynomial function in the unknown parameters $\kappa_1,\kappa_2,\kappa_3,\kappa_4$ whose coefficients depend on the collected data. Physically the parameters are all positive real numbers, i.e., $0<\kappa_i<\infty$ for all i so the minimum value of $E_p^2(\kappa_1,\kappa_2,\kappa_3,\kappa_4)$ must be in this open set and thus occurs

at an extremum value. Consequently, the minimum value must satisfy the extrema equations. Computing

$$r_i(\kappa_1,\kappa_2,\kappa_3,\kappa_4) \triangleq \partial E_p^2(\kappa_1,\kappa_2,\kappa_3,\kappa_4)/\partial\kappa_i = 0$$

for all i results in

$$\begin{aligned}
r_1(\kappa_1,\kappa_2,\kappa_3,\kappa_4) &= -2R_{Wy1} - 2R_{Wy5}\kappa_2 + 2R_{W11}\kappa_1 \\
&\quad + 2R_{W12}\kappa_2 + 2R_{W13}\kappa_3 + 2R_{W14}\kappa_4 \\
&\quad + 4R_{W15}\kappa_1\kappa_2 + 2R_{W25}\kappa_2^2 + 2R_{W35}\kappa_2\kappa_3 \\
&\quad + 2R_{W55}\kappa_1\kappa_2^2 \\
r_2(\kappa_1,\kappa_2,\kappa_3,\kappa_4) &= -2R_{Wy2} - 2R_{Wy5}\kappa_1 + 2R_{W12}\kappa_1 \\
&\quad + 2R_{W22}\kappa_2 + 2R_{W23}\kappa_3 + 2R_{W15}\kappa_1^2 \\
&\quad + 4R_{W25}\kappa_1\kappa_2 + 2R_{W35}\kappa_1\kappa_3 + 2R_{W55}\kappa_1^2\kappa_2 \\
r_3(\kappa_1,\kappa_2,\kappa_3,\kappa_4) &= -2R_{Wy3} + 2R_{W13}\kappa_1 + 2R_{W23}\kappa_2 \\
&\quad + 2R_{W33}\kappa_3 + 2R_{W35}\kappa_1\kappa_2 \\
r_4(\kappa_1,\kappa_2,\kappa_3,\kappa_4) &= -2R_{Wy4} + 2R_{W14}\kappa_1 + 2R_{W44}\kappa_4.
\end{aligned} \tag{27}$$

This is a set of four polynomials in the four unknowns κ_1, κ_2, κ_3, κ_4, and the table below lists the degree of each polynomial with respect to each of the unknown parameters.

TABLE I
D-AXIS POLYNOMIAL DEGREES

	deg κ_1	deg κ_2	deg κ_3	deg κ_4
r_1	1	2	1	1
r_2	2	1	1	0
r_3	1	1	1	0
r_4	1	0	0	1

Algebraic elimination theory (from Algebraic Geometry [41]–[43]) provides a systematic procedure to solve these equations for *all* possible solutions.[1] There can only be a finite number of solutions and thus one simply substitutes each solution into $E_p^2(\kappa_1,\kappa_2,\kappa_3,\kappa_4)$ to determine which one corresponds to the *global* minimum. The resulting algorithm is therefore non-iterative in contrast to iterative techniques that rely on Newton's method, for example, to find the minima of a given error function.

The elimination steps that were carried out (one of several possible elimination scenarios) are summarized as follows:

1) Eliminate κ_4 from r_1, r_2, r_3, r_4, to get the polynomials $p_{12}(\kappa_1,\kappa_2,\kappa_3)$, $p_{13}(\kappa_1,\kappa_2,\kappa_3)$, $p_{14}(\kappa_1,\kappa_2,\kappa_3)$.
2) Eliminate κ_3 from p_{12}, p_{13}, p_{14}, to get the polynomials $p_{1213}(\kappa_1,\kappa_2)$, $p_{1214}(\kappa_1,\kappa_2)$.
3) Eliminate κ_2 from p_{1213}, p_{1214}, to get the polynomial $p_{121314}(\kappa_1)$.

These resultant polynomials are then solved in reverse order starting with p_{121314}, followed by p_{1213}, p_{1214}, then p_{12}, p_{13}, p_{14} and finally r_1, r_2, r_3, r_4. Note that the c's in the following polynomials represent their coefficients. The resultant polynomial $p_{121314}(\kappa_1)$ has the form

$$\begin{aligned}
p_{121314}(\kappa_1) &= c_{1,6}\kappa_1^6 + c_{1,5}\kappa_1^5 + c_{1,4}\kappa_1^4 + c_{1,3}\kappa_1^3 \\
&\quad + c_{1,2}\kappa_1^2 + c_{1,1}\kappa_1 + c_{1,0}
\end{aligned} \tag{28}$$

[1]See p. 565 of [44] for a short tutorial on elimination theory using resultants.

where $c_{1,i}$ for $i = 0$ to 6 are computed using the elements of R_W and R_{Wy}. This polynomial has six possible solutions for κ_1, so each valid (real and positive) solution is saved and used to solve the subsequent polynomials. For each valid solution κ_1, the following polynomials are solved for κ_2

$$p_{1213}(\kappa_2) = c_{2,1}(\kappa_1)\kappa_2 + c_{2,0}(\kappa_1) \tag{29}$$

$$p_{1214}(\kappa_2) = c_{3,2}(\kappa_1)\kappa_2^2 + c_{3,2}(\kappa_1)\kappa_2^2 + c_{3,0}(\kappa_1) \tag{30}$$

The coefficients are functions of the value of κ_1 obtained from (28). There is only one valid solution κ_2 for each solution κ_1 because p_{1213} is a first order polynomial in κ_2. If neither of the two solutions κ_2 of p_{1214} matches the solution of p_{1213}, or if that solution is invalid then the corresponding κ_1 is invalid. Otherwise, the pair (κ_1,κ_2) is saved and used as a possible solution in the subsequent computations.

For each of the valid solutions (κ_1,κ_2), the following polynomials are solved for κ_3

$$p_{12}(\kappa_3) = c_{4,1}(\kappa_1,\kappa_2)\kappa_3 + c_{4,0}(\kappa_1,\kappa_2) \tag{31}$$

$$p_{13}(\kappa_3) = c_{5,1}(\kappa_1,\kappa_2)\kappa_3 + c_{5,0}(\kappa_1,\kappa_2) \tag{32}$$

$$p_{14}(\kappa_3) = c_{6,1}(\kappa_1,\kappa_2)\kappa_3 + c_{6,0}(\kappa_1,\kappa_2). \tag{33}$$

For each valid (κ_1,κ_2) there is only one possible value of κ_3, which is the same for all three polynomials p_{12}, p_{13}, p_{14}. If that is the case and it is a valid solution, the set $(\kappa_1,\kappa_2,\kappa_3)$ is used in the subsequent computations.

The remaining polynomials are

$$r_1(\kappa_4) = c_{7,1}(\kappa_1,\kappa_2,\kappa_3)\kappa_4 + c_{7,0}(\kappa_1,\kappa_2,\kappa_3) \tag{34}$$

$$r_4(\kappa_4) = c_{8,1}(\kappa_1,\kappa_2,\kappa_3)\kappa_4 + c_{8,0}(\kappa_1,\kappa_2,\kappa_3) \tag{35}$$

Note that r_2, r_3 are not polynomials in κ_4, as seen in Table I.

The resulting valid solution sets $(\kappa_1,\kappa_2,\kappa_3,\kappa_4)$ are substituted into $E_p^2(\kappa_1,\kappa_2,\kappa_3,\kappa_4)$ of (26) to determine which one yields the lowest error, and consequently corresponds to the global minimum. This solution is directly related to L_{AD}, L'_F, r'_{Rd}, and L'_{Rd}, see equation (22).

B. Identification of q-axis parameters

Similarly, for the q-axis, we re-write (19) in regressor form as

$$y_q = W_q K_q \tag{36}$$

where

$$y_q \triangleq \frac{dv_{Sq}}{dt} + r_S\frac{di_{Sq}}{dt} + L_{lS}\frac{d^2i_{Sq}}{dt^2},$$

$$W_q \triangleq \begin{bmatrix} -\dfrac{d^2i_{Sq}}{dt^2} & -v_{Sq} - r_S i_{Sq} - L_{lS}\dfrac{di_{Sq}}{dt} \\ \dfrac{d^2i_{Sq}}{dt^2} & -\dfrac{di_{Sq}}{dt} \end{bmatrix},$$

$$\begin{aligned}
K_q &= \begin{bmatrix} \kappa_6 & \kappa_7 & \kappa_8 & \kappa_9 \end{bmatrix}^T \\
&\triangleq \begin{bmatrix} L_{AQ} & \dfrac{r'_{Rq}}{L'_{Rq}} & L_{AQ}^2\dfrac{1}{L'_{Rq}} & L_{AQ}\dfrac{r'_{Rq}}{L'_{Rq}} \end{bmatrix}^T.
\end{aligned} \tag{37}$$

As in the case for the d-axis, both y_q and W_q are known, whereas K_q contains the unknown parameters. Also, the

regressor is overparameterized because $\kappa_9 = \kappa_6\kappa_7$. The parameter set K_q will be estimated by choosing the value that minimizes

$$E_q^2(K_q) = R_y - R_{Wy}^T K_q - K_q^T R_{Wy} + K_q^T R_W K_q \quad (38)$$

where

$$R_y \triangleq \sum_{n=1}^{N} y_q^T(nT) y_q(nT),\ R_W \triangleq \sum_{n=1}^{N} W_q^T(nT) W_q(nT),$$
$$R_{Wy} \triangleq \sum_{n=1}^{N} W_q^T(nT) y_q(nT). \quad (39)$$

and as with the d-axis parameters case, R_W is singular.

A nonlinear (in the parameters) identification model is developed by substituting for the constraint $\kappa_9 = \kappa_6\kappa_7$ in the error function

$$\begin{aligned} & E_p^2(\kappa_6, \kappa_7, \kappa_8) \quad (40) \\ = \ & R_y - 2R_{Wy}^T K_q\big|_{\kappa_9=\kappa_6\kappa_7} + K_q^T R_W K_q\big|_{\kappa_9=\kappa_6\kappa_7}. \end{aligned}$$

The resulting error function is then differentiated with respect to each of the independent parameters κ_6, κ_7, κ_8 to get three polynomials, namely, $r_5(\kappa_6, \kappa_7, \kappa_8)$, $r_6(\kappa_6, \kappa_7, \kappa_8)$, and $r_7(\kappa_6, \kappa_7, \kappa_8)$. The following table lists the degrees of these polynomials with respect to the unknown parameters.

TABLE II
Q-AXIS POLYNOMIAL DEGREES

	deg κ_6	deg κ_7	deg κ_8
r_5	1	2	1
r_6	2	1	1
r_7	1	1	1

To solve them using elimination theory, we first eliminate κ_8 from r_5, r_6, r_7, to get the polynomials $p_{12}(\kappa_6, \kappa_7)$, $p_{13}(\kappa_6, \kappa_7)$. Then, eliminate κ_6 from p_{12}, p_{13}, to get the polynomial $p_{1213}(\kappa_7)$. The resultant polynomials are solved in reverse order, starting with p_{1213}, then p_{12}, p_{13}, then finally r_5, r_6, r_7. These polynomials have the form

$$\begin{aligned} p_{1213}(\kappa_7) &= c_{1,6}\kappa_7^6 + c_{1,5}\kappa_7^5 + c_{1,4}\kappa_7^4 + c_{1,3}\kappa_7^3 \quad (41) \\ &\quad + c_{1,2}\kappa_7^2 + c_{1,1}\kappa_7 + c_{1,0} \\ p_{12}(\kappa_6) &= c_{2,2}(\kappa_7)\kappa_6^2 + c_{2,1}(\kappa_7)\kappa_6 + c_{2,0}(\kappa_7) \quad (42) \\ p_{13}(\kappa_6) &= c_{3,1}(\kappa_7)\kappa_6 + c_{3,0}(\kappa_7) \quad (43) \\ r_5(\kappa_8) &= c_{4,1}(\kappa_6, \kappa_7)\kappa_8 + c_{4,0}(\kappa_6, \kappa_7) \quad (44) \\ r_6(\kappa_8) &= c_{5,1}(\kappa_6, \kappa_7)\kappa_8 + c_{5,0}(\kappa_6, \kappa_7) \quad (45) \\ r_7(\kappa_8) &= c_{6,1}(\kappa_6, \kappa_7)\kappa_8 + c_{6,0}(\kappa_6, \kappa_7) \quad (46) \end{aligned}$$

where the c's are the coefficients of the polynomials.

These solution sets $(\kappa_6, \kappa_7, \kappa_8)$ are substituted into $E_p^2(\kappa_6, \kappa_7, \kappa_8)$ of (40) to determine which one yields the lowest error, and therefore corresponds to the global minimum. The q-axis parameters L_{AQ}, r'_{Rq}, and L'_{Rq} are directly related to this solution set, see equation (37).

C. An error index

After estimating the parameters using an identification technique it is useful to have a metric to compare the results. One such metric, known as an error index, is defined in this section (see Ch. 2 of [44]). The least squared error was given in (24) and (38) as

$$E^2(K) = R_y - R_{Wy}^T K - K^T R_{Wy} + K^T R_W K.$$

Let K^* denote the parameter vector that minimizes the error function $E^2(K)$. Then, the error index is defined as (see [44])

$$EI \triangleq \sqrt{\frac{E^2(K)\big|_{K=K^*}}{E^2(K)\big|_{K=\mathbf{0}}}} \leq 1. \quad (47)$$

This error index should be significantly less than 1 to indicate that there is an improvement in taking the parameter vector of the model to be K^* over taking $K = 0$! If a complete nominal set of parameter values K_{nom} is available then the ratio $\sqrt{E^2(K^*)/E^2(K_{nom})}$ might be of more interest.

IV. Experimental Setup and Results

The offline identification technique was implemented experimentally on a 120 VA two pole pairs ($n_p = 2$) salient rotor synchronous generator with damper bars, namely, the EMS8241 by LabVolt. The salient pole rotor and the damper bars is a small scale version of a large salient pole generator in that they both can be modelled using the same electrical model in Section II.

This section outlines the experimental setup, the preparatory measurements and experiments required to determine the values of r_S, r_F, L_{lS}, and N_{afd}, and the offline identification experiment that estimates the remaining electrical parameters.

A. Experimental setup

The experimental setup is comprised of the EMS8241 synchronous machine, the HP 6834 B programmable three phase power supply, current and voltage measurement transducers, an analog filtering stage, the NI-PCI E-series data acquisition board, and a PC, as depicted in Fig. 2.

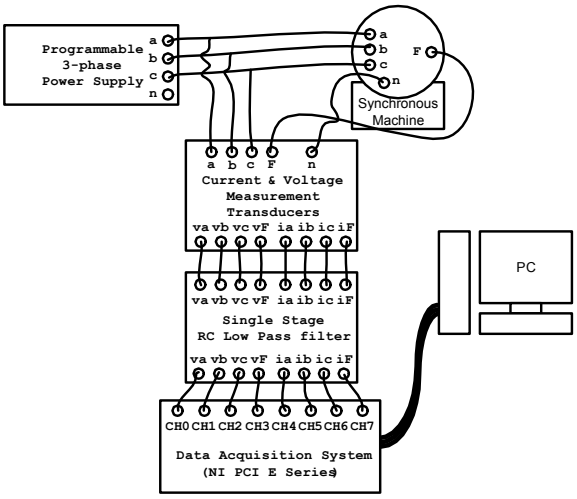

Fig. 2. A schematic of the experimental setup for the offline test.

The power supply produces a set of balanced three-phase voltages, with the capability of ramping up the voltage amplitude and frequency of the waveforms. The current and voltage measurement transducers were custom built with the capability of simultaneously measuring four voltage signals and four current signals. These transducers produce voltage signals that are filtered using a first-order low-pass Butterworth filter, implemented via an RC circuit, with a cut-off frequency of $f_c \approx 720$ Hz. The filtered signals are then sampled at a frequency $f_S = 10$ kHz using the data acquisition board.

B. Preparatory experiments

A few DC measurements and experiments were carried out to obtain the electrical parameters required by the offline identification model. Specifically, DC measurements were conducted for the stator resistance, and the field resistance, which were found to be $r_S = 11.75\ \Omega$, and $r_F = 121.5\ \Omega$, respectively (the nominal values being $r_S = 12.5\ \Omega$ and $r_F = 120\ \Omega$). Two experiments were carried out to determine the stator leakage inductance L_{lS} and the scaling factor N_{afd}.

1) The unbalanced stator voltage experiment - determining L_{lS} : Parameter identification techniques typically rely on the manufacturer supplied stator leakage inductance, see for example [1], and [5]. Aliprantis et al. [40] computed L_{lS} from SSFR test data using Genetic Algorithms. Here a simple test to determine a value for L_{lS} was carried out by applying the same sinusoidal voltage source to all three stator phases, with an rms voltage of V_S so that

$$\begin{aligned} v_S &= v_a = v_b = v_c = \sqrt{2} V_S \sin(\omega_S t), \\ i_S &= i_a + i_b + i_c. \end{aligned}$$

With the stator windings connected in a Y configuration, the source is connected between the a, b, c terminals (shorted together) and their neutral n terminal. By the transformation in (7) we have

$$\begin{aligned} v_0 &= \sqrt{3}\sqrt{2} V_S \sin(\omega_S t), \\ v_{Sd} &= v_{Sq} = 0, \\ i_{Sd} &= i_{Sq} = 0. \end{aligned}$$

Furthermore, with the field winding open-circuited, i.e., $i_F = 0$, the model of the machine from (1)–(6) reduces to equation (1), with $v_0 = \sqrt{3} v_S$ and $i_0 = i_S/\sqrt{3}$, we have

$$3 v_S = -r_S i_S - L_{lS} \frac{d i_S}{dt}.$$

By measuring the rms magnitudes V_S and I_S of v_S and i_S, respectively, we have

$$L_{lS} = \sqrt{\left((3V_S/I_S)^2 - r_S^2 \right) / \omega_S^2}. \tag{48}$$

In the test that was carried out, several values for V_S and I_S were applied and measured. With $r_S = 11.75\ \Omega$, and $\omega_S = 2\pi \times 60$ rad/s, the averaged value for the stator leakage inductance from six trials is $L_{lS} = 16.2$ mH. This is lower than the manufacturer supplied value of $L_{lS} = 49.3$ mH.

2) The open-circuit no-load test - determining N_{afd}: Identification techniques rely on the scaling factor

$$N_{afd} \triangleq \sqrt{\frac{2}{3}} \frac{N_F}{N_S}$$

that is obtained from the no-load magnetization curve, see [1], [27], [38]. This test requires the generator to be operated at no load, with an open-circuited stator, and a field current applied while the stator voltage is measured. It can be shown, see Ch. 2 of [39], that under these conditions the scaling factor is given by

$$N_{afd} \triangleq \sqrt{\frac{2}{3}} \frac{N_F}{N_S} = \sqrt{3} \frac{v_{a,rms}}{\omega_S i_F L_{AD}}. \tag{49}$$

Using the manufacturer supplied value of the d-axis stator self inductance $L_{Sd} = 126/\omega_S = 0.3342$ H, and the previously computed stator leakage inductance $L_{lS} = 16.2$ mH, the mutual inductance used for this computation is

$$L_{AD} = L_{Sd} - L_{lS} = 0.3180 \text{ H}.$$

The values of N_{afd} are tabulated below.

TABLE III
EXPERIMENTAL RESULTS FOR THE SCALING FACTOR N_{aF}

	Trial 1	Trial 2	Trial 3
Stator phase voltage v_a (V_{rms})	14.1	28.1	53
Field current i_F (A_{dc})	0.05	0.1	0.2
Scaling factor N_{afd}	4.1	4.1	3.8

The average of these values was taken to be the scaling factor $N_{afd} = 4.0$. As we shall see later (see also Ch. 6 of [39]) $L_{AD} = 0.3180$ H and N_{afd} were iterated through our identification algorithm until they converged to a consistent pair of values in the sense that one yields the other.

C. The offline standstill experiment

The offline standstill identification model was used to estimate the electrical parameters of the machine, namely, L_{AD}, L_{AQ}, L'_F, L'_{Rd}, L'_{Rq}, r'_{Rd}, and r'_{Rq}. The identification method requires that the rotor of the generator be locked at an arbitrary, but known, rotor angle. Then a balanced three-phase chirp voltage waveform is applied to the stator for a short time to excite the machine. The field winding is short-circuited (i.e., $v_F = 0$) and the measured signals are v_a, v_b, v_c, i_a, i_b, i_c, and i_F.

The procedure for conducting the offline standstill experiment entails programming the voltage supply to generate the test signals, determining the rotor angle θ, recording v_a, v_b, v_c, i_a, i_b, i_c, and i_F, and applying the offline identification algorithm to compute the parameters.

1) The voltage test signals: A set of balanced 3-phase sinusoidal chirp test voltage signals were generated for 8 seconds with their frequency increased linearly from 45 to 85 Hz. The operating frequency of 60 Hz lies within this range, however, this selection is not a requirement of the identification method. The amplitude of the voltage signals was increased for the first 4 seconds from 0 to 30 V_{rms}, and then held at that value to the end of the test. Low

test voltage and current levels are a requirement for offline standstill techniques.

Note that the SSFR test [2] requires a starting frequency of 1 mHz. Therefore, higher-end equipment is required to generate noise free signals at these low frequencies. For example, the HP 6834 B cannot start the frequency sweep below 40 Hz.

2) Determining the rotor angle θ: The rotor angle could be determined using an absolute position encoder that keeps track of the rotor's angular displacement with respect to the a-axis. Another approach, used in this experiment, is to align the d-axis of the rotor with the a-axis of the stator so that $\theta = 0$ rad, and lock it in position. A DC source is used to establish positive currents i_a and i_F flowing *into* terminals a' and F respectively, see Fig. 1.

3) Data collection: The signals were captured for the experiments in a window of 12 s, larger than the test period, to allow the operator sufficient time for triggering. The captured signals are shown in the following figures.

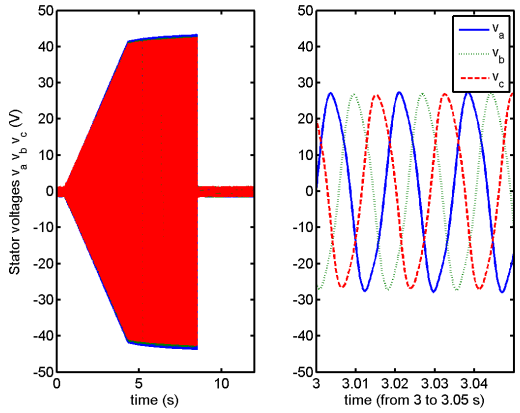

Fig. 3. Stator voltages v_a, v_b, v_c vs time - the offline experiment.

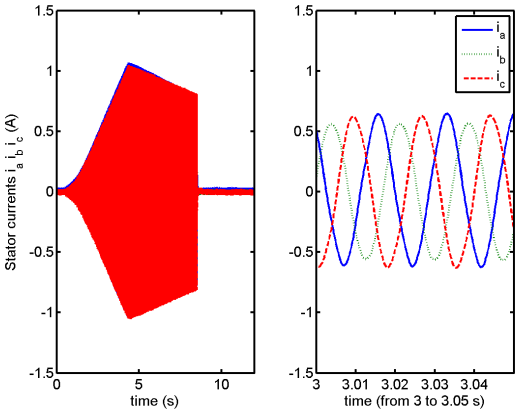

Fig. 4. Stator currents i_a, i_b, i_c vs time - the offline experiment.

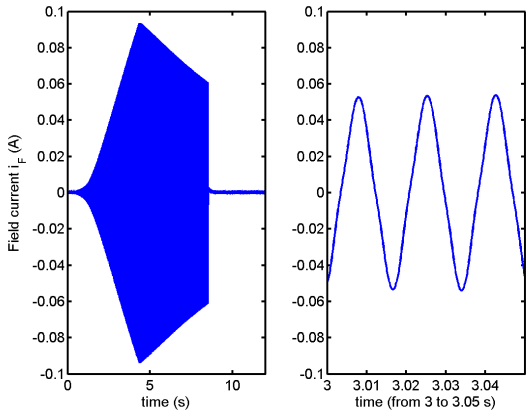

Fig. 5. Field current i_F vs time - the offline experiment.

4) Offline identification algorithm: The data captured in each experiment is then used by the offline identification algorithm to find the set of parameters that best fit the model of the machine. Recall that the identification models of the *d* and *q* axes are decoupled, resulting in two sets of identification model parameters,

$$K_d^T = \left[L_{AD} \quad \frac{r'_{Rd}}{L'_{Rd}} \quad L_{AD}^2 \frac{1}{L'_{Rd}} \quad L'_F \quad L_{AD} \frac{r'_{Rd}}{L'_{Rd}} \right],$$

$$K_q^T = \left[L_{AQ} \quad \frac{r'_{Rq}}{L'_{Rq}} \quad L_{AQ}^2 \frac{1}{L'_{Rq}} \quad L_{AQ} \frac{r'_{Rq}}{L'_{Rq}} \right].$$

Following is a summary of the steps carried out by the identification algorithm:

1) The signals v_a, v_b, v_c, i_a, i_b, i_c, i_F, (and $v_F = 0$) are filtered using a discrete-time 4^{th} order low pass Butterworth filter implemented using the `filtfilt` command in MATLAB with a cut-off frequency of $f_c = 200$ Hz. This filtering is particularly important because first and second order differentiation is applied to the measured variables. The trade-off in choosing the order of the filter and the cut-off frequency is between eliminating the measurement noise and retaining the information contained in the signals.
2) The signal i_F is scaled by N_{afd} to give i'_F, using the relationship $i'_F = N_{afd} i_F$.
3) The abc to $0dq$ coordinate transformation of (7) is applied to the stator signals with $\theta = 0$.
4) The derivatives are computed using the center difference numerical differentiation method. For any signal $x(t)$, e.g., $x(t) = i_{Sd}(t)$ they are computed as

$$\left.\frac{dx}{dt}\right|_{t=nT} \approx \frac{x\left((n+1)T\right) - x\left((n-1)T\right)}{2T}$$

$$\left.\frac{d^2x}{dt^2}\right|_{t=nT} \approx \frac{x\left((n+1)T\right) + x\left((n-1)T\right) - 2x\left(nT\right)}{T^2}$$

where n is the time index of the discrete-time signal, and the sampling period $T = 1/f_S = 0.1$ ms.
5) A time range of data is selected by the user from the available data, in this case $t = 2$ to 8 s. Hence, the

discrete time index $n = 1$ to N corresponds to the selected time range. This step is carried out to eliminate the ranges where the signals have measurement noise, i.e., a relatively low signal-to-noise (SNR) ratio.

6) For each data point, $n = 1$ to N, we compute $y_d(nT)$, $W_d(nT)$ from (21) and $y_q(nT)$, $W_q(nT)$ from (36).
7) The matrices and vectors R_y, R_{Wy}, and R_W are then computed by summing up all the data points from $n = 1$ to N using (25) for the the d-axis, and (39) for the the q-axis. These are used in computing the coefficients of the polynomials.
8) The polynomials (28)–(35) are solved for a finite number of roots $(\kappa_1, \kappa_2, \kappa_3, \kappa_4)$, and the solution that results in the lowest error when substituted in $E_p^2(\kappa_1, \kappa_2, \kappa_3, \kappa_4)$ of (26) is selected. Also, polynomials (41)–(46) are solved for the root $(\kappa_6, \kappa_7, \kappa_8)$ that minimizes $E_p^2(\kappa_6, \kappa_7, \kappa_8)$ of (40).
9) The parameters of the machine are simply computed using the relationships

$$\begin{aligned} L_{AD} &= \kappa_1, L_{AQ} = \kappa_6, L'_F = \kappa_4, L'_{Rd} = \kappa_1^2/\kappa_3, \\ L'_{Rq} &= \kappa_6^2/\kappa_8, r'_{Rd} = \kappa_2\kappa_1^2/\kappa_3, r'_{Rq} = \kappa_7\kappa_6^2/\kappa_8. \end{aligned}$$

10) The error indices for the d and q-axis parameters are computed using (47).

5) Results of the offline identification experiments: The offline identification algorithm was carried out on the collected experimental data. The algorithm used the preparatory experiment parameters $r_S = 11.75\ \Omega$, $r_F = 121.5\ \Omega$, $L_{lS} = 16.2$ mH, and $N_{afd} = 4$. The nominal parameters (resistances and unsaturated inductances) supplied by the manufacturer[2] are $r_S = 12.5\ \Omega$, $r_F = 120\ \Omega$, $L_{lS} = 49.3$ mH, $L_{AD} = 0.285$ H, and $L_{AQ} = 0.277$ H. The estimated parameters are given in the Table IV, with the error indices computed as $EI_{d-axis} = 0.1179$, and $EI_{q-axis} = 0.0924$.

TABLE IV
RESULTS OF THE OFFLINE IDENTIFICATION METHOD

Parameter	L_{AD} (H)	L_{AQ} (H)	L'_F (H)	L'_{Rd} (H)
Value	0.2260	0.2140	0.4976	0.3246
Parameter	L'_{Rq} (H)	r'_{Rd} (Ω)	r'_{Rq} (Ω)	
Value	0.2899	50.1121	32.8429	

6) Simulations versus experimental results: In addition to quantitative metrics, like the error index, the efficacy of the identification algorithm can be demonstrated qualitatively by simulating the mathematical model using the estimated parameters with the recorded experimental voltage signals as input, and then comparing the resulting current waveforms with the recorded ones. The experimental versus simulated currents are shown for i_a and i'_F in the following plots. The results show a close match between the experimental waveforms and the simulated waveforms. Recall that the test voltage signals were sweeping frequencies from 45Hz to 85Hz, over a time range of $t \approx 0.5$ to 8.5 s, whereas the data used by the offline parameter identification algorithm was a subset of that time range.

[2]These parameters are supplied by the manufacturer as the reference values to which they build the EMS 8241 120/208 V – 60 Hz, synchronous machine. Therefore, they were not supplied as accurate measurements of the parameters of the specific machine used in the experiments presented in this work.

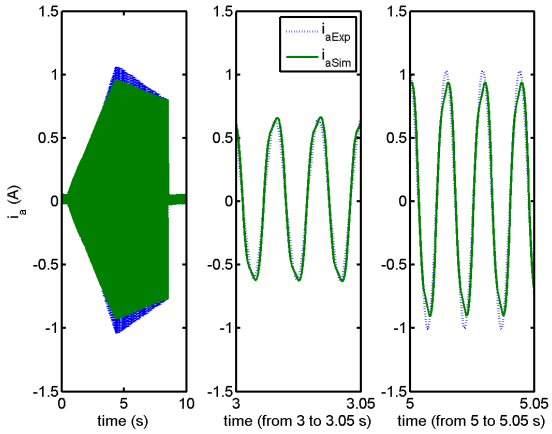

Fig. 6. Stator current i_a - simulation vs experiment data.

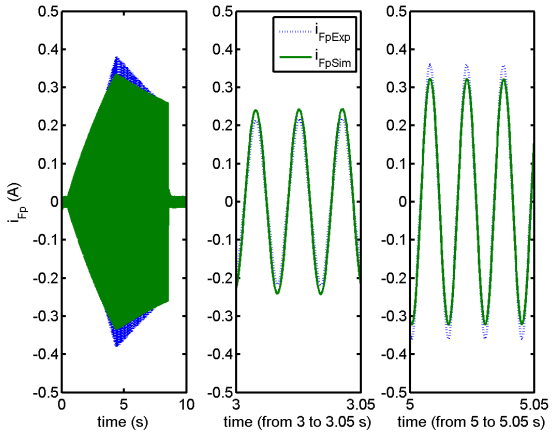

Fig. 7. Field current i'_F - simulation vs experiment data.

7) Scale Factor N_{afd}: In practice [1] and in this work, N_{afd} is obtained using (49) and relies on an initial estimate of $L_{AD} = 0.3180$ H. The following iterative procedure is not necessary, however, it shows that successively applying the identification algorithm starting from $N_{afd} = 4.0$ to compute L_{AD} then using it to recompute N_{afd} and so on converges to a consistent pair (i.e., one yields the other). Specifically, the procedure converges to the parameter values given in Table V. See [39] for more elaboration.

TABLE V
PARAMETER VALUES AFTER CONVERGENCE OF N_{afd} AND L_{AD}

Parameter	L_{AD} (H)	L_{AQ} (H)	L'_F (H)	L'_{Rd} (H)
Value	0.2616	0.2140	0.4850	0.3592
Parameter	L'_{Rq} (H)	r'_{Rd} (Ω)	r'_{Rq} (Ω)	N_{afd}
Value	0.2899	51.9894	32.8429	4.944

The error indices are $EI_{d-axis} = 0.1144$ and $EI_{q-axis} = 0.0924$. Comparing Table V with Table IV it is seen that *only* the converged values N_{afd} and L_{AD} are significantly different.

V. Acknowledgement

The first author is grateful for the financial support provided by Alfaisal University through grant IRG201150101142.

VI. Conclusion

An offline parameter estimation method was developed and proposed for large synchronous machines that are represented by Model 2.1 in IEEE 1110-2002 [1]. The methodology developed here requires less than 10 seconds of data, and guarantees to minimize a global least-squares error criterion to furnish the electrical parameters of the machine.

The advantages of this method over the standard SSFR test [2] include having a significantly shorter test time, seconds versus hours, and the utilization of equipment with a smaller frequency range. This was due to the fact that the method requires capturing transient data, whereas the SSFR test requires steady state data obtained at different frequencies from 10 mHz to over 100 Hz. In addition, aligning the rotor of large machines as required by the standard SSFR test [2] can be challenging. This is avoided by extensions of the SSFR test in [9], [10] and again in this work by allowing for an arbitrary rotor angle position. On the other hand, using the frequency response obtained from the SSFR test one can determine the appropriate number of damper windings in each axis. In the method presented here that functionality is yet to be developed.

The method was conducted experimentally on a small salient-pole synchronous machine with squirrel-cage damper bars, which is represented by Model 2.1. An error index was defined which gave a relative indication on how well the estimated parameters fit the data. Also, a comparison of experimentally recorded waveforms versus simulation waveforms (using the same inputs) showed that both sets of signals were in phase and very close in magnitude. Both of these measures demonstrated the success of this method in predicting the electrical parameters of the machine. These results support the proposal of implementing this method on large synchronous machines. Future work can investigate different model structures using the standstill technique, e.g., for round-rotor synchronous generators, in addition to other types of electric machines.

References

[1] IEEE, Park Avenue, NY, *IEEE Guide for Synchronous Generator Modeling Practices and Applications in Power System Stability Analyses*, 2002.

[2] IEEE, New York, NY, *IEEE Guide: Test Procedures for Synchronous Machines*, 1995.

[3] Western Systems Coordinating Council, Salt Lake City, UT, *Test Guidelines for Synchronous Unit Dynamic Testing and Model Validation*, 1997.

[4] J. Apt, L. B. Lave, S. Talukdar, M. G. Morgan, and M. Ilic, "Electrical blackouts: A systemic problem", *Issues in Science and Technology*, vol. 20, no. 4, pp. 55–61, 2004.

[5] Paul C. Krause, *Analysis of Electric Machinery*, McGraw-Hill, New York, 1986.

[6] P. Sauer and M. Pai, *Power System Dynamics and Stability*, Stipes Publishing, Champaign, IL, 2007.

[7] O. Touhami, H. Guesbaoui, and C. Iung, "Synchronous machine parameter identification by a multitime scale technique", *IEEE transactions on industry applications*, vol. 30, no. 6, pp. 1600–1608, 1994.

[8] D.C. Aliprantis, S.D. Sudhoff, and B.T. Kuhn, "A synchronous machine model with saturation and arbitrary rotor network representation", *IEEE Transactions on Energy Conversion*, vol. 20, no. 3, pp. 584–594, September 2005.

[9] E. da Costa Bortoni and J. A. Jardini, "A standstill frequency response method for large salient pole synchronous machines", *IEEE Transactions on energy conversion*, vol. 19, no. 4, pp. 687–691, 2004.

[10] F. K. Dalton and A. W. W. Cameron, "Simplified measurement of subtransient reactances in synchronous machines", *Electrical Engineering*, vol. 71, no. 2, pp. 167–170, 1952.

[11] Paul C. Krause, Oleg Wasynczuk, and Scott D. Sudhoff, *Analysis of Electric Machinery and Drive Systems*, 2nd Edition, John Wiley & Sons, New York, 2002.

[12] F.P. de Mello and L.N. Hannett, "Determination of synchronous machine electrical characteristics by test", *IEEE Transactions on Power Apparatus and Systems*, vol. PAS-102, no. 12, pp. 3810–3815, December 1983.

[13] P.A.E. Rusche, G.J. Brock, L.N. Hannett, and J.R. Willis, "Test and simulation of network dynamic response using ssfr and rtdr derived synchronous machine models", *IEEE Transactions on Energy Conversion*, vol. 5, no. 1, pp. 145–155, March 1990.

[14] I Kamwa, P Viarouge, and E. J. Dickinson, "Identification of generalised models of synchronous machines from time-domain tests", *IEE Proceedings C (Generation, Transmission and Distribution)*, vol. 138, no. 6, pp. 485–498, 1991.

[15] A. Tumageanian, A. Keyhani, S.I. Moon, T. Leksan, and L. Xu and, "Maximum likelihood estimation of synchronous machine parameters from flux decay data", *IEEE Transactions on Industry Applications*, vol. 30, no. 2, pp. 433–439, 1994.

[16] A. Tumageanian and A. Keyhani, "Identification of synchronous machine linear parameters from standstill step voltage input data", *IEEE Transactions on Energy Conversion*, vol. 10, no. 2, pp. 232–240, 1995.

[17] M. Cisneros-Gonzalez, C. Hernandez, R. Morales-Caporal, E. Bonilla-Huerta, and M. A. Arjona, "Parameter estimation of a synchronous-generator two-axis model based on the standstill chirp test", *IEEE Transactions on Energy Conversion*, vol. 28, no. 1, pp. 44–51, 2013.

[18] P.L. Dandeno, P. Kundur, A.T. Poray, and H.M. Zein El-Din, "Adaptation and validation of turbogenerator model parameters through on-line frequency response measurements", *IEEE Transactions on Power Apparatus and Systems*, vol. PAS-100, no. 4, pp. 1656–1664, April 1981.

[19] H. Tsai, A. Keyhani, J. Demcko, and R.G. Farmer, "On-line synchronous machine parameter estimation from small disturbance operating data", *IEEE Transactions on Energy Conversion*, vol. 10, no. 1, pp. 25–36, March 1995.

[20] R. Wamkeue, I. Kamwa, X. Dai-Do, and A. Keyhani, "Iteratively reweighted least squares for maximum likelihood identification of synchronous machine parameters from on-line tests", *IEEE Transactions on Energy Conversion*, vol. 14, no. 2, pp. 159–166, 1999.

[21] A. Mohamed, A. Hussain, S.M. Zali, and A. Ariffin, "A systematic approach in estimating the generator parameters", *Electric Power Components and Systems*, vol. 30, no. 3, pp. 301–313, mar 2002.

[22] M. Burth, G. Verghese, and M. Velez-Reyes, "Subset selection for improved parameter estimation in on-line identification of a synchronous generator", *IEEE Transactions on Power Systems*, vol. 14, no. 1, pp. 218–225, 1999.

[23] Miguel Vélez-Reyes, *Decomposed algorithms for parameter estimation*, PhD thesis, Massachusetts Institute of Technology, 1992.

[24] Miguel Vélez-Reyes, W. L. Fung, and J. E. Ramos-Torres, "Developing robust algorithms for speed and parameter estimation in induction machines", in *Proceedings of the IEEE Conference on Decision and Control*, 2001, pp. 2223–2228, Orlando, Florida.

[25] M. Vélez-Reyes, K. Minami, and G. Verghese, "Recursive speed and parameter estimation for induction machines", in *Proceedings of the IEEE Industry Applications Conference*, 1989, pp. 607–611, San Diego, California.

[26] H. Karayaka, A. Keyhani, G. Heydt, B. Agrawal, and D. Selin, "Synchronous generator model identification and parameter estimation from operating data", *IEEE Transactions on Energy Conversion*, vol. 18, no. 1, pp. 121–125, 2003.

[27] E. Kyriakides, *Innovative Concepts for On-line Synchronous Generator Parameter Estimation*, PhD thesis, Arizona State University, 2003.

[28] John Chiasson, Kaiyu Wang, Mengwei Li, Marc Bodson, and Leon M. Tolbert, "Algebraic methods for nonlinear systems: Parameter identification and state estimation", in *Current Trends in Nonlinear Systems and Control*. Laura Menini, Luca Zaccarian and Chaouki T. Abdallah, Eds., 2005, pp. 57–76, Birkhäuser.

[29] John Chiasson and Marc Bodson, "Estimation of the rotor time constant of an induction machine at constant speed", in *Proceedings of the European Control Conference ECC'07*, July 2-5 2007, pp. 4673–4678, Kos Greece.

[30] Kaiyu Wang, John Chiasson, Marc Bodson, and Leon M. Tolbert, "A nonlinear least-squares approach for estimation of the induction motor parameters", in *Proceedings of the IEEE Conference on Decision and Control*, December 2004, pp. 3856–3861.

[31] Kaiyu Wang, John Chiasson, Marc Bodson, and Leon M. Tolbert, "Tracking the rotor time constant of an induction motor traction drive for HEVs", in *Proceedings of the IEEE Workshop on Power Electronics in Transportation (WPET)*, October 2004, pp. 83–88.

[32] Kaiyu Wang, John Chiasson, Marc Bodson, and Leon M. Tolbert, "An on-line rotor time constant estimator for the induction machine", in *Proceedings of the IEEE International Electric Machines and Drives Conference*, May 2005, pp. 608–614, San Antonio TX.

[33] Kaiyu Wang, John Chiasson, Marc Bodson, and Leon Tolbert, "A nonlinear least-squares approach for estimation of the induction motor parameters", *IEEE Transactions on Automatic Control*, vol. 50, no. 10, pp. 1622–1628, October 2005.

[34] Kaiyu Wang, John Chiasson, Marc Bodson, and Leon M. Tolbert, "An on-line method for tracking the rotor time constant of an induction machine", in *Proceedings of the 2005 American Control Conference*, June 2005, pp. 2739–2744, Portland, Oregon.

[35] Kaiyu Wang, John Chiasson, Marc Bodson, and Leon Tolbert, "An online rotor time constant estimator for the induction machine", *IEEE Transactions on Control Systems Technology*, vol. 15, no. 2, pp. 339–348, March 2007.

[36] Ahmed Oteafy, John Chiasson, and Said Ahmed-Zaid, "A standstill parameter identification technique for the synchronous generator", in *Proceedings of the International Electric Machines and Drives Conference*, May 10-13 2015, Coeur d'Alene, Idaho, USA.

[37] A. R. Bergen, *Power Systems Analysis*, 1st Edition, Prentice-Hall, Englewood Cliffs, NJ, 1986.

[38] Paul M. Anderson and A. A. Fouad, *Power System Control and Stability*, IEEE Press, 1994.

[39] A. Oteafy, *Novel Parameter Identification Techniques for Large Synchronous Generators*, PhD thesis, Boise State University, 2011.

[40] D.C. Aliprantis, S.D. Sudhoff, and B.T. Kuhn, "Experimental characterization procedure for a synchronous machine model with saturation and arbitrary rotor network representation", *IEEE Transactions on Energy Conversion*, vol. 20, no. 3, pp. 595–603, September 2005.

[41] Joachim von zur Gathen and Jürgen Gerhard, *Modern Computer Algebra*, Cambridge University Press, Cambridge, UK, 1999.

[42] David Cox, John Little, and Donal O'Shea, *IDEALS, VARIETIES, AND ALGORITHMS An Introduction to Computational Algebraic Geometry and Commutative Algebra*, 2nd Edition, Springer-Verlag, Berlin, 1996.

[43] David Cox, John Little, and Donal O'Shea, *Using Algebraic Geometry*, Springer-Verlag, Berlin, 1998.

[44] John Chiasson, *Modeling and High-Performance Control of Electric Machines*, John Wiley & Sons, 2005.